DALTON
FULL PAPER

Structural, spectroscopic and electrochemical studies of binuclear nickel(II) complexes of bis(pentadentate) ligands derived from bis(1,4,7-triazacyclononane) macrocycles

Suzanne J. Brudenell,[a] Leone Spiccia,*[a] Alan M. Bond,[a] Peter C. Mahon[a] and David C. R. Hockless[b]

[a] *Department of Chemistry, Monash University, Clayton, Victoria 3168, Australia. E-mail: leone.spiccia@sci.monash.edu.au*
[b] *Research School of Chemistry, Australian National University, Canberra, ACT 2601, Australia*

Received 3rd August 1998, Accepted 9th October 1998

Binuclear nickel(II) complexes of bis(pentadentate) ligands generated by functionalisation of the four secondary nitrogens in bis(tacn) macrocycles with 2-pyridylmethyl arms have been prepared, isolated and characterised. The pentadentate compartments are linked by $(CH_2)_2$ {tmpdtne, $[Ni_2(tmpdtne)(OH_2)_2][ClO_4]_4 \cdot 5H_2O$ **1**}, $(CH_2)_3$ {tmpdtnp, $[Ni_2(tmpdtnp)(OH_2)_2][ClO_4]_4$ **2**}, $(CH_2)_4$ {tmpdtnb, $[Ni_2(tmpdtnb)(OH_2)_2][ClO_4]_4$ **3**}, $CH_2C_6H_4CH_2$-*m* {tmpdtn*m*-X, $[Ni_2(tmptdtm\text{-}X)(OH_2)_2][ClO_4]_4 \cdot 3H_2O$ **4**} and $CH_2CHOHCH_2$ {tmpdtnp-OH, $[Ni_2(tmpdtnp\text{-}OH)(OH_2)_2][ClO_4]_4$ **5**} bridging units. Single crystal X-ray diffraction studies of **3** have confirmed that each nickel(II) centre is in a distorted octahedral geometry defined by five N-donors from a pentadentate compartment of the ligand and an oxygen donor from a water ligand. Tetragonal elongation of the geometry is evidenced by the axial Ni–N distances, which are *ca.* 0.05 Å longer than the three equatorial Ni–N distances. The two pentadentate compartments are oriented in an *anti* configuration with the two aqua ligands pointing away from each other. Cyclic and square-wave voltammetric studies on **1**–**5** indicate that the complexes undergo oxidation to the nickel(III) state in two overlapping $1e^-$ processes (*i.e.* $Ni^{II}NI^{II} \longrightarrow Ni^{II}Ni^{III} \longrightarrow Ni^{III}Ni^{III}$). Two partially resolved $1e^-$ oxidation waves were observed for **1** and **5** while for **2**–**4** two $1e^-$ processes were indicated by fact that the signals were broader than expected for a single $2e^-$ process.

Introduction

Nickel is recognised as an essential trace element for bacteria, plants and animals.[1–4] The active sites of enzymes such as urease, carbon monoxide dehydrogenase, [NiFe]-hydrogenase and methyl-S-coenzyme-M methylreductase are known to contain nickel centres, which are intimately involved in the catalytic cycles.[5] Until the recent reports of the structures of urease[6] and [NiFe]-hydrogenase,[7] X-ray structural data on nickel-enzymes was lacking. The quest for information about the structures and modes of action of nickel active sites continues to generate interest in the development of synthetic models for the various nickel biosites and in the co-ordination chemistry of nickel in general.[5,8–13] Apart from their potential to form the basis of models for the polynuclear active sites of Ni containing enzymes, complexes of macrocyclic ligands and their derivatives are ideal for studying magnetic exchange interactions[9,10] and the redox properties of nickel(II) centres in close proximity.[11]

Ciampolini *et al.*[11] recognised the potential for homo-bimetallic complexes of bis(macrocyclic) ligands to be ideal models for the study of mutual electrostatic effects in two-centre redox systems. Accordingly, a number of binuclear nickel(II) complexes based on bis(cyclam) ligands were synthesized in which the Ni···Ni separation could be tuned through the use of aliphatic and aromatic bridges of varying length. Electrochemical studies of the stepwise two-electron oxidation of these dinickel(II) complexes revealed that, as the metal–metal separation increased, a reduction in electrostatic repulsion between proximal nickel(II) centres facilitated the oxidation of the complexes. Investigations of the corresponding bis(tacn) macrocycles (tacn = 1,4,7-triazacyclononane) have revealed that the ethane-linked bis(tacn) ligand, dtne, forms exclusively the mononuclear nickel(II) sandwich complex and there was no evidence for formation of the binuclear compound, even when an excess of nickel(II) salt was used.[12] In contrast, the *o*-xylene bridged bis(macrocycle) is able to behave as either a hexadentate ligand, co-ordinating to one Ni^{II}, or as a bis(tridentate) ligand, co-ordinating to two Ni^{II} while the *m*- and *p*-xylene bridged ligands yield only the binuclear complex.[13] Although these types of bis(tacn) ligands have for example, been applied successfully in the synthesis of bridged binuclear copper complexes and in reactivity studies related to oxygen transport and activation by binuclear copper biosites[14] few attempts have been made to prepare bridged binuclear nickel complexes. One exception is the use of a novel bis(Me_2tacn)calix[4]arene ligand which, by virtue of the calixarene linking unit, formed a unique ferromagnetic binuclear nickel(II) complex bridged by three azide ligands co-ordinating in the end-on mode.[9]

Apart from a binuclear complex incorporating a bis(tacn) ligand with alcohol pendant arms,[15] no other nickel(II) complexes of bis(tacn) ligands with potentially co-ordinating pendant arms have been described. We have recently reported two series of bis(pentadentate) ligands, obtained by attaching either 2-pyridylmethyl[16,17] or acetate[18] pendant groups to each secondary nitrogen in bis(tacn) macrocycles, and the corresponding binuclear copper(II) complexes. The complexes of ligands bearing 2-pyridylmethyl arms were found to exhibit interesting variations in spectroscopic and electrochemical properties with Cu···Cu separation tunable by the type of spacer used. We report here the synthesis and characterisation of the first series of binuclear nickel(II) complexes of bis(pentadentate) ligands incorporating 2-pyridylmethyl pendant arms (Scheme 1).

Experimental

Materials and reagents

Reagent or AR grade materials were used throughout the study. The ligands 1,2-bis[4,7-bis(2-pyridylmethyl)-1,4,7-triazacyclonon-1-yl]ethane (tmpdtne),[16] 1,3-bis[4,7-bis(2-pyridyl-

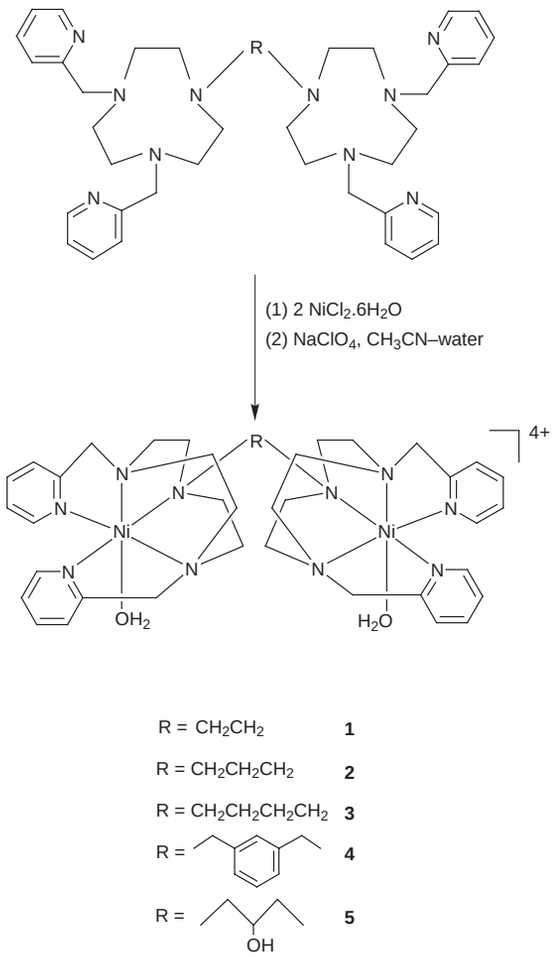

R = CH_2CH_2 **1**

R = $CH_2CH_2CH_2$ **2**

R = $CH_2CH_2CH_2CH_2$ **3**

R = **4**

R = **5**

Scheme 1

methyl)-1,4,7-triazacyclonon-1-yl]propane (tmpdtnp),[16] 1,4-bis[4,7-bis(2-pyridylmethyl)-1,4,7-(triazacyclonon-1-yl]butane (tmpdtnb),[16] 1,3-[4,7-bis(2-pyridylmethyl)-1,4,7-triazacyclonon-1-ylmethyl]benzene (tmpdtn*m*-X)[17] and 1,3-bis[4,7-bis(2-pyridylmethyl)-1,4,7-triazacyclonon-1-yl]propan-2-ol (tmpdtnp-OH)[17] were all prepared by published methods.

Physical measurements

Infrared spectra were measured on a Perkin-Elmer 1600 FTIR spectrometer as KBr pellets or Nujol mulls, and electronic spectra on a Cary 5G spectrometer. Electron microprobe analyses were made with a JEOL JSM-1 scanning electron microscope through an NEC X-ray detector and pulse processing system connected to a Packard multichannel analyser. Microanalyses were performed by Chemical and Micro-Analytical Services (CMAS) of Melbourne, Australia. Room temperature magnetic moments were determined by the Faraday method. Diamagnetic corrections were made using Pascal's constants. Cyclic (scan rate 100 mV s^{-1}) and square-wave (period 30 ms) voltammograms were recorded in dry, nitrogen degassed acetonitrile solutions (≈0.5 mmol dm^{-3}) with tetrabutylammonium perchlorate (0.1 mol dm^{-3}) as the supporting electrolyte on a Cypress CS 1090 system connected to a platinum macrodisc working electrode ($r = 0.8$ mm), platinum auxiliary electrode and $Ag–Ag^+$ (10 mmol dm^{-3} $AgNO_3$) reference. The voltammetrically reversible oxidation of ferrocene (Fc) was used as an internal standard and potentials are reported relative to the $Fc–Fc^+$ couple.

CAUTION: Although no problems were encountered in this work, transition metal perchlorates are potentially explosive. They should be prepared in small quantities and handled with care.

Synthesis of complexes

$[Ni_2(tmpdtne)(OH_2)_2][ClO_4]_4·5H_2O$ 1. To a dark red-brown solution of tmpdtne (1.70 g, 2.62 mmol) in ethanol (20 cm^3) was added a slight excess of $NiCl_2·6H_2O$ (1.31 g, 5.51 mmol). The resulting brown solution was diluted with water (1 dm^3) and loaded on to a Sephadex SP-C25 cation-exchange column. After washing the column thoroughly with distilled water two bands were visible. The first, faint pink, corresponded to $[Ni(tacntmp)]Cl_2$ impurity and was eluted with a 0.1 mol dm^{-3} $NaClO_4$ aqueous solution. The major pink band, corresponding to the desired binuclear nickel(II) complex, was eluted with a 1 mol dm^{-3} $NaClO_4$ solution consisting of a 70:30 mixture of water and CH_3CN. Acetonitrile was added to prevent the complex from crystallising on the resin. Following elution, the solution was concentrated yielding a pink solid. In some syntheses sodium perchlorate was added to enhance precipitation. This was recrystallised from a CH_3CN–water mixture to give a pink-purple crystalline product (yield 1.72 g, 55%) {Found: C, 35.3; H, 5.2; N, 10.9. Calc. for $[Ni_2C_{38}H_{52}N_{10})(OH_2)_2][ClO_4]_4·5H_2O$: C, 35.4; H, 5.1; N, 10.9%}. Electron microprobe: Cl:Ni ratio 2:1. Selected IR bands (KBr, cm^{-1}): 3418 (br), 2930m, 1608s, 1467m, 1448w, 1088vs, 768m and 629s. Magnetic moment: μ_{eff} (292 K) = 2.81 μ_B per Ni^{II}.

$[Ni_2(tmpdtnp)(OH_2)_2][ClO_4]_4$ 2. The procedure used to prepare complex **1** was followed except for tmpdtnp (1.10 g, 1.67 mmol) and $NiCl_2·6H_2O$ (0.83 g, 3.50 mmol). Recrystallisation from a CH_3CN–water mixture gave a purple crystalline solid (yield 1.05 g, 52%) {Found: C, 36.6; H, 5.0; N, 10.8. Calc. for $[Ni_2(C_{39}H_{54}N_{10})(OH_2)_2][ClO_4]_4$: C, 36.6; H, 4.5; N, 11.0%}. Electron microprobe: Cl:Ni ratio 2:1. Selected IR bands (KBr, cm^{-1}): 3421 (br), 2928w, 1609m, 1467s, 1447m, 1088vs, 767m and 627s. Magnetic moment: μ_{eff} (295 K) = 2.91 μ_B per Ni^{II}.

$[Ni_2(tmpdtnb)(OH_2)_2][ClO_4]_4$ 3. The procedure used to prepare complex **1** was followed except for tmpdtnb (1.00 g, 1.49 mmol) and $NiCl_2·6H_2O$ (0.74 g, 3.13 mmol). Purple crystals suitable for X-ray crystallography were grown from a CH_3CN–water mixture (yield 1.01 g, 57%). {Found: C, 40.0; H, 4.8; N, 11.5. Calc. for $[Ni_2(C_{40}H_{56}N_{10})(OH_2)_2][ClO_4]_4$: C, 39.1; H, 4.9; N, 11.4%}. Electron microprobe: Cl:Ni ratio 2:1. Selected IR bands (KBr, cm^{-1}): 3419 (br), 2932m, 1609s, 1468m, 1445m, 1090vs, 767m and 628s. Magnetic moment: μ_{eff} (295 K) = 2.98 μ_B per Ni^{II}.

$[Ni_2(tmpdtn$*m*$-X)(OH_2)_2][ClO_4]_4·3H_2O$ 4. The procedure used to prepare complex **1** was followed except for tmpdtn*m*-X (2.06 g, 2.85 mmol) and $NiCl_2·6H_2O$ (1.42 g, 5.98 mmol). A pink crystalline solid was obtained after recrystallisation from a CH_3CN–water mixture (yield 1.21 g, 32%) {Found: C, 39.7; H, 4.8; N, 10.6. Calc. for $[Ni_2(C_{44}H_{56}N_{10})(OH_2)_2][ClO_4]_4·3H_2O$: C, 39.7; H, 5.0; N, 10.5%}. Electron microprobe: Cl:Ni ratio 2:1. Selected IR bands (KBr, cm^{-1}): 3432 (br), 2930w, 1608s, 1470m, 1446m, 1093vs, 764m and 626s. Magnetic moment: μ_{eff} (295 K) = 2.98 μ_B per Ni^{II}.

$[Ni_2(tmpdtnp-OH)(OH_2)_2][ClO_4]_4$ 5. The procedure used to prepare complex **1** was followed except for tmpdtnp-OH (1.10 g, 1.62 mmol) and $NiCl_2·6H_2O$ (0.81 g, 3.41 mmol). The product appeared as a pink crystalline solid after recrystallisation from a CH_3CN–water mixture (yield 0.66 g, 33%). {Found: C, 37.7; H, 5.0; N, 11.7. Calc. for $[Ni_2(C_{39}H_{53}N_{10}OH)(OH_2)_2][ClO_4]_4$: C, 38.0; H, 4.7; N, 11.4%}. Electron microprobe: Cl:Ni ratio 2:1. ESI Mass spectrum: $[Ni_2L(ClO_4)_3]^+$, *m*/*z* 1094.0; $[Ni_2L(ClO_4)_2]^{2+}$ 497.2; $[Ni_2L(ClO_4)]^{3+}$, 298.6. Selected IR bands (KBr, cm^{-1}): 3508 (br), 3100m, 2939m, 1610s, 1470s, 1448s, 1095vs, 766s and 625s. Magnetic moment: μ_{eff} (292 K) = 2.99 μ_B per Ni^{II}.

Table 1 Crystallographic data for $[Ni_2(tmpdtnb)(OH_2)_2][ClO_4]_4$ **3**

Formula	$C_{40}H_{60}Cl_4N_{10}Ni_2O_{18}$
M	1228.18
Crystal system	Triclinic
Space group	$P\bar{1}$ (no. 2)
a/Å	9.562(4)
b/Å	10.414(4)
c/Å	14.171(4)
α/°	82.97(4)
β/°	79.65(3)
γ/°	66.34(4)
U/Å^3	1270(1)
Z	1
T/K	293(1)
D_c/g cm^{-3}	1.606
μ(Mo-Kα)/cm^{-1}	10.35
$2\theta_{max}$/°, hkl data collected	50.1, $+h$, $\pm k$, $\pm l$
No. data measured	4798
No. unique data	4501
No. observed data [$I \geq 3\sigma(I)$]	3084
R	0.048
R'	0.035

Crystallography

Intensity data for a purple plate crystal of complex **3** of dimensions $0.28 \times 0.24 \times 0.06$ mm were measured on a Rigaku AFC6S diffractometer fitted with graphite-monochromated Mo-Kα radiation. Cell constants and the orientation matrix for data collection were obtained from a least-squares refinement using the setting angles of 18 carefully centered reflections in the range $11.85 < 2\theta < 18.67°$. The ω–2θ scan technique to a maximum 2θ value of 50.1° was used to collect 4798 (4501 unique) reflections from which 3084 with $I \geq 3.0\sigma(I)$ were used in the refinement. The intensities of three representative reflections were measured after every 150 and no decay correction was applied. The data were corrected for Lorentz-polarisation effects[19] and an empirical absorption correction was applied.[20] The structure was solved by direct methods[21] and expanded using Fourier techniques in the DIRDIF 94 program.[22] All non-hydrogen atoms were refined anisotropically. Hydrogen atoms were included in calculated positions and not refined. The final cycle of full-matrix least-squares refinement was based on F. Neutral atom scattering factors were taken from ref. 23 and anomalous dispersion effects[24] were included in F_{calc}. Calculations were performed using the TEXSAN crystallographic software package.[25] Crystallographic data are given in Table 1.

CCDC reference number 186/1196.

Results and discussion

Synthesis

The binuclear nickel(II) complexes of tmpdtne, tmpdtnp, tmpdtnb, tmpdtn*m*-X and tmpdtnp-OH were all prepared by treating ethanolic solutions of the 'free' ligands with an excess of $NiCl_2 \cdot 6H_2O$ (Scheme 1). Cation exchange chromatography of the reaction mixtures yielded a major pink band, on elution with water–acetonitrile mixture containing 1 mol dm^{-3} $NaClO_4$, from which the diaqua forms of the binuclear nickel(II) complexes could be crystallised. Satisfactory elemental analyses were obtained for all five complexes and electron microprobe analysis indicated a uniform Ni : Cl ratio of 1 : 2. The IR spectra showed bands indicative of the presence of the ligands and counter ions. The ESI mass spectrum of **5** confirmed the presence of species with composition $[Ni_2L(ClO_4)_3]^+$, $[Ni_2L(ClO_4)_2]^{2+}$ and $[Ni_2L(ClO_4)]^{3+}$. This indicated that deprotonation of the propan-2-ol ligand backbone did not occur and hence that the formation of an endogenously bridged binuclear complex was unlikely.

Table 2 Selected bond distances (Å) and angles (°) for $[Ni_2(tmpdtnb)(OH_2)_2][ClO_4]_4$ **3**

Ni–O(1)	2.095(3)	N(2)–C(3)	1.473(6)
Ni–N(1)	2.134(4)	N(3)–C(13)	1.479(6)
Ni–N(2)	2.066(4)	N(3)–C(4)	1.500(6)
Ni–N(3)	2.085(4)	N(3)–C(5)	1.479(6)
Ni–N(4)	2.082(4)	N(2)–C(7)	1.477(6)
Ni–N(5)	2.107(4)	N(4)–C(8)	1.344(6)
N(1)–C(1)	1.477(6)	N(4)–C(12)	1.330(6)
N(1)–C(6)	1.502(6)	N(5)–C(14)	1.345(6)
N(2)–C(2)	1.506(6)	N(5)–C(18)	1.336(6)
O(1)–Ni–N(1)	94.8(1)	O(1)–Ni–N(2)	174.8(2)
O(1)–Ni–N(3)	100.3(2)	O(1)–Ni–N(4)	93.8(2)
O(1)–Ni–N(5)	86.1(1)	N(1)–Ni–N(2)	85.1(2)
N(1)–Ni–N(3)	83.8(2)	N(1)–Ni–N(4)	98.3(2)
N(1)–Ni–N(5)	164.0(2)	N(2)–Ni–N(3)	84.9(2)
N(2)–Ni–N(4)	81.1(2)	N(2)–Ni–N(5)	95.5(2)
N(3)–Ni–N(4)	165.6(2)	N(3)–Ni–N(5)	80.3(2)
N(4)–Ni–N(5)	97.6(2)	Ni–N(1)–C(1)	102.2(3)
Ni–N(1)–C(6)	107.5(3)	C(1)–N(1)–C(6)	111.5(4)
Ni–N(2)–C(2)	108.8(3)	Ci–N(2)–C(3)	105.5(3)
Ni–N(3)–C(13)	106.0(3)	C(2)–N(2)–C(3)	111.5(4)
C(2)–N(2)–C(7)	106.3(3)	C(3)–N(2)–C(7)	112.6(4)
Ni–N(3)–C(4)	108.7(3)	Ni–N(3)–C(5)	104.6(3)
Ni–N(3)–C(13)	106.0(3)	C(4)–N(3)–C(5)	112.3(4)
C(4)–N(3)–C(13)	112.1(4)	C(5)–N(3)–C(13)	112.7(4)
Ni–N(4)–C(8)	112.5(3)	Ni–N(4)–C(12)	129.1(4)
C(8)–N(4)–C(12)	118.4(5)	Ni–N(5)–C(14)	112.7(3)
Ni–N(5)–C(18)	129.5(4)	C(14)–N(5)–C(18)	117.8(5)

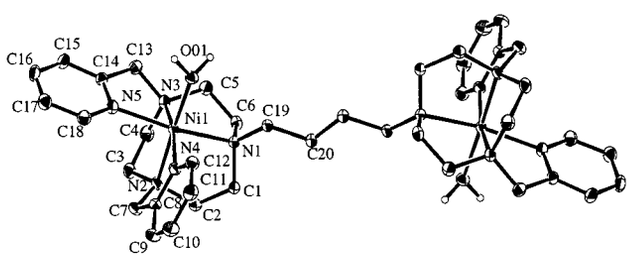

Fig. 1 An ORTEP[26] plot of $[Ni_2(tmpdtnb)(OH_2)_2][ClO_4]_4$ **3** (thermal ellipsoids are drawn at 30%).

Crystal structure of $[Ni_2(tmpdtnb)(OH_2)_2][ClO_4]_4$ 3

The molecular structure of the cation in complex **3** is shown in Fig. 1. Each nickel(II) centre is in a distorted octahedral geometry defined by five N atoms from the ligand and an oxygen donor from an H_2O ligand. The N(1) and N(5) nitrogens form the axial bonds with an average bond length of 2.12 Å, while the N(2), N(3), N(4) and O(1) donor atoms comprise the equatorial bonds with a shorter average length of 2.08 Å. As is observed in the analogous copper(II) complexes,[16,17] the M–N distance to the bridgehead nitrogen, *viz.* the Ni–N(1) bond of 2.134(4) Å, is longer than the equatorial Ni–N (tacn) distances of 2.066(4) [Ni–N(2)] and 2.085(4) Å [Ni–N(3)] (Table 2). This difference, however, is smaller than in the copper(II) complexes.[16,17]

Although the Ni–N (py) axial bond length of 2.107(4) Å [Ni–N(5)] is marginally longer than the Ni–N (py) equatorial bond distance of 2.082(4) Å [Ni–N(4)], these distances are typical for nickel(II) complexes of pyridyl arm bearing tacn derivatives.[10,27–29] The remaining Ni–O(1) equatorial bond of 2.095(3) Å is similar to the Ni–O distance of 2.10 Å in $[Ni(py_2\text{-}tasn)(H_2O)][ClO_4]_2$ [py_2-tasn = 4,7-bis(2-pyridylmethyl)-1-thia-4,7-diazacyclononane].[27] The two pentadentate compartments of the ligand in **3** are oriented away from each other in an *anti* configuration, as was found for the manganese(II) analogue[30] and the nickel(II) complex of a related ligand with alcohol pendant arms.[15] However, **3** shows considerably less distortion from regular octahedral geometry than the manganese(II) complex, *viz.* the N(1)–Ni–N(5), O(1)–Ni–N(2) and N(3)–Ni–N(4) angles of 164.0(2), 174.8(2) and 165.6(2)° in **3** are closer to the

Table 3 UV-Visible spectral data of **1**–**5**[a] and some related nickel(II) complexes

Complex	λ_{max}/nm (ε_{max}/dm^3 mol^{-1} cm^{-1})	Ref.
1	519 (42), 812 (64), 878 (sh) (42)	This work
2	524 (36), 811 (63), 878 (sh) (40)	This work
3	519 (39), 812 (64), 878 (sh) (42)	This work
4	519 (35), 806 (60), 881 (sh) (44)	This work
5	524 (39), 820 (58), 894 (sh) (44)	This work
[Ni(dmptacn)-(OH_2)][ClO_4]$_2$[a]	516 (18), 800 (23), 880 (sh) (22)	10
[Ni(tmptacn)]-[ClO_4]$_2$[a]	515 (27), 810 (36), 886 (sh) (24)	36
[Ni(dtne)][ClO_4]$_2$[b]	363 (16), 516 (18), 848 (31), 917 (31)	12
[Ni(tacn)$_2$]Cl_2[b]	310 (12), 500 (9), 800 (9), 870 (sh)	37
[Ni(tatacn)][ClO_4]$_2$[b]	355 (18), 557 (13), 805 (17), 924 (34)	28, 29

dmptacn = 1,4-bis(2-pyridylmethyl)-1,4,7-triazacyclononane; tmptacn = 1,4,7-tris(2-pyridylmethyl)-1,4,7-triazacyclononane; dtne = 1,2-bis(1,4,7-triazacyclonon-1-yl)ethane; tatacn = 1,4,7-triazacyclononane-*N*,*N*′,*N*″-triacetate. [a] In CH_3CN. [b] In water.

expected value of 180° than the corresponding angles in the manganese(II) complex, which are in the 140–160° range.[30] Furthermore, the tacn N–Ni–N chelate angles in **3** (average 84.6°) are much closer to 90° than the corresponding N–Mn–N angles (average 76.0°).[30]

The Ni···Ni′ separation of 9.563(4) Å in complex **3** is 1.284 Å longer than that observed in the corresponding manganese(II) analogue.[30] This is predominantly a consequence of the orientation of the two halves of the complex around the bridgehead nitrogens. In **3** the Ni–N(1)–C(19)–C(20) and Ni′–N(1′)–C(19′)–C(20′) torsion angles, which are a measure of the orientation of pentadentate compartments relative to the axis of the bridging group, are −10.9(8) and +169.1(8)°, respectively while in the manganese(II) complex they are +59.6(8) and −59.5(8)°. Although both complexes adopt *anti* configurations, the arrangement of the bridging unit is much more linear in **3**. This can be seen in the extended cell diagram for **3** and may explain the longer M···M separation when compared with the manganese(II) complex. It is notable that the Cu···Cu distance in the copper(II) complex of the same bis(pentadentate) ligand is also much shorter (by 0.88 Å[17]) than that in **3**. Molecular modelling calculations on this copper(II) complex and those of the other bis(pentadentate) ligands shown in Scheme 1 have predicted that these complexes can adopt a number of configurations, which differ only in the relative orientation of the pentadentate compartments, with similar strain energies in solution.[17] Under these circumstances, it is not surprising to find that variations in crystal packing effects that result from changes in the metal centre can be responsible for significant variations in solid state structures.

Electronic spectra and magnetic behaviour

The UV-Visible spectral data for complexes **1**–**5** recorded in acetonitrile are summarised in Table 3. Two of the three spin allowed transitions expected for Ni^{II} in a near octahedral ligand field[31,32] were observed [$^3A_{2g} \longrightarrow {}^3T_{2g}$ (800–900), $^3A_{2g} \longrightarrow {}^3T_{1g}$(F) (500–550 nm)] but the third transition [$^3A_{2g} \longrightarrow {}^3T_{1g}$(P)] normally found in the 300–400 nm region is masked by $\pi \longrightarrow \pi^*$ and/or CT transitions involving the pyridine rings. The band in the 800–900 nm region, corresponding to the $^2A_{2g} \longrightarrow {}^3T_{2g}$ transition, is asymmetric as highlighted by a shoulder at *ca.* 880 nm for each complex. Such behaviour is also evident in the related octahedral nickel(II) complexes mentioned in Table 3 and may be attributed to low symmetry splitting or spin–orbit splitting of the $^3T_{2g}$ state, or the close approach of the ^1E_g state such that the spin forbidden $^3A_{2g} \longrightarrow {}^1E_g$ transition gains intensity through spin–orbit coupling with the $^3T_{2g}$ state.[32,33]

There is little difference in the λ_{max} values for complexes **1**–**4** which range from 519 to 524, 806 to 812 and a shoulder at 878 to 881 nm. However, the values for **5**, in which the two halves of the ligand are joined by a propan-2-ol bridge, are the highest in the series. This indicates that the tmpdtnp-OH ligand exerts a weaker ligand field than the other ligands, possibly due to the electron withdrawing power of the OH group. The fact that the absorption maxima for all the complexes **1**–**5** are at lower energy than those for [Ni(dmptacn)(OH_2)][ClO_4]$_2$ indicates that the bis(pentadentate) ligands exert a weaker ligand field than does dmptacn. This lower ligand field can be attributed to the presence of an extra tertiary nitrogen per pentadentate compartment in the binucleating ligands.

The effective magnetic moments, μ_{eff} (per Ni^{II}), of complexes **1**–**5** at room temperature range from 2.81 to 2.99 μ_B. On average these values are slightly higher than the spin-only value due to second order spin–orbit coupling effects but they are typical for nickel(II) amine complexes in an octahedral environment.

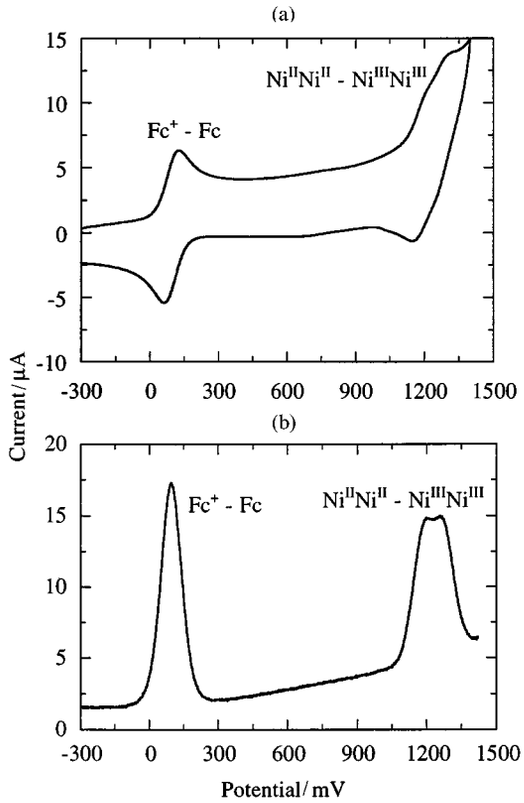

Fig. 2 Cyclic (scan rate = 100 mV s^{-1}) (a) and square-wave (period = 30 ms) (b) voltammograms of complex **1** in acetonitrile (0.1 mol dm^{-3} Bu_4NClO_4) using a platinum macrodisc electrode at 20 °C. The potential axis used is relative to the Ag–Ag^+ reference.

Electrochemistry

The redox behaviour of the binuclear nickel(II) complexes, **1**–**5**, has been studied by cyclic and square-wave voltammetry (SWV) at a platinum macroelectrode. The CV and SWV traces of **1**, shown in Fig. 2, are composed of two partially resolved signals, but clearly indicate that oxidation of the two nickel(II) centres to Ni^{III} occurs at slightly different potentials, eqn. (1).

$$Ni^{II}Ni^{II} + e^- \rightleftharpoons Ni^{III}Ni^{II} + e^- \rightleftharpoons Ni^{III}Ni^{III} \quad (1)$$

The potentials for the two oxidation processes for the binuclear nickel complexes are so positive that the second process overlaps with the onset of the background process. Consequently, cyclic voltammetric experiments involve switching the potential in a region where highly reactive species are produced by oxidation of the solvent (electrolyte). It is believed that it is the reaction of these solvent derived species with the dinickel(III) complex which lead to an apparently significant level of

Table 4 Cyclic and square-wave voltammetric data for oxidation of nickel(II) complexes in acetonitrile (0.1 mol dm^{-3} Bu_4NClO_4)[a]

Complex	Cyclic[b]				Square wave[c]		
	$E_{\frac{1}{2}}$/V	ΔE_p/mV	E_p^{ox}/V	E_p^{red}/V	E_p/V	$W_{\frac{1}{2}}$[d]/mV	I_p/μA
Fc	0.00	58	−0.03	+0.03	0.00	100	14.9
1	+1.11	96	+1.16	+1.06	+1.11	120[e]	7.9
	+1.17	96	+1.22	+1.12	+1.17	120[e]	7.7
2	+1.07	84	+1.11	+1.03	+1.07	110	14.2
3	+1.06	80	+1.10	+1.02	+1.06	110	15.2
4	+1.11	86	+1.15	+1.07	+1.11	100	15.2
5	+1.06	55	+1.08	+1.03	+1.07	150[e]	8.9
	+1.17	41	+1.19	+1.15	+1.17	150[e]	7.0

[a] Potentials are quoted with respect to the Fc–Fc^+ couple used as an internal reference. The concentrations of the complexes used were in the range 0.5–0.55 mmol dm^{-3} but the current data are normalised to 0.5 mmol dm^{-3} to facilitate comparison of values. [b] Cyclic voltammetric data were obtained at a scan rate of 100 mV s^{-1}. The close proximity of the background process and the interference this causes with the voltammetry of the binuclear nickel complexes (see text) means that peak currents for the reduction component on the reverse scan of the CV experiment are perturbed. Consequently, ratios of oxidation and reduction peak heights for nickel processes, usually calculated to assess their chemical reversibility, cannot be obtained for this system. [c] Square-wave voltammetric data were measured with a period of 30 ms. [d] $W_{\frac{1}{2}}$ is the estimated width of the peak shaped process response at half the wave height. [e] Inadequate resolution available to provide values for individual processes. Numbers given refer to the width of the total response.

chemical irreversibility being associated with the cyclic voltammetric response for the binuclear nickel processes. That is, it is this reaction and not any inherent instability of $Ni^{III}Ni^{III}$ on the CV timescale which leads to the observation of unequal peak heights of the oxidation and reduction components of the nickel oxidation processes. In addition to precluding the assessment of the chemical reversibility of the two oxidation processes, the proximity to the background process prevents well resolved limiting current values being obtained under steady state conditions *via* the use of microdisc or rotated disc electrodes, as was possible with the binuclear copper-systems. However, fortunately, the square wave technique only requires the measurement of data obtained from scanning the potential in the positive direction and adequate resolution can be obtained from the background response with this technique. Consequently, the SWV method can be used to obtain quantitatively useful data.

The $E_{\frac{1}{2}}$ values, +1.11 and +1.17 V (Table 4), estimated from both techniques, confirm that a potential separation of approximately 60 mV exists for the two oxidation processes of compound **1**. This finding indicates that the metal centres are close enough electronically to influence one another so that, once the first nickel(II) centre has been oxidised to Ni^{III}, the second becomes more difficult to oxidise due to the additional positive charge that has been introduced.[34] This behaviour is also evident in the oxidation of the analogous manganese(II) complex, where two partially resolved oxidation processes are observed in forming the $Mn^{III}Mn^{III}$ state,[30] but not in reduction of the corresponding copper(II) complex, where a decrease in electrostatic repulsion between the two copper centres may occur on reduction to the $Cu^{I}Cu^{I}$ state.[17] Notably, Ciampolini *et al.*[11] have reported that oxidation of the nickel(II) complex of the ethane linked bis(cyclam) ligand also occurs in two even more clearly distinguishable processes whose reversible potentials are separated by 100 mV.

The CV and SWV responses of the nickel(II) complex of tmpdtnp-OH, **5**, displayed in Fig. 3, are similar to those of **1** in that they are broadened and clearly composed of two partially resolved oxidation processes. Nevertheless, despite problems associated with incomplete resolution and proximity to the solvent limit, analysis of data obtained from both the CV and

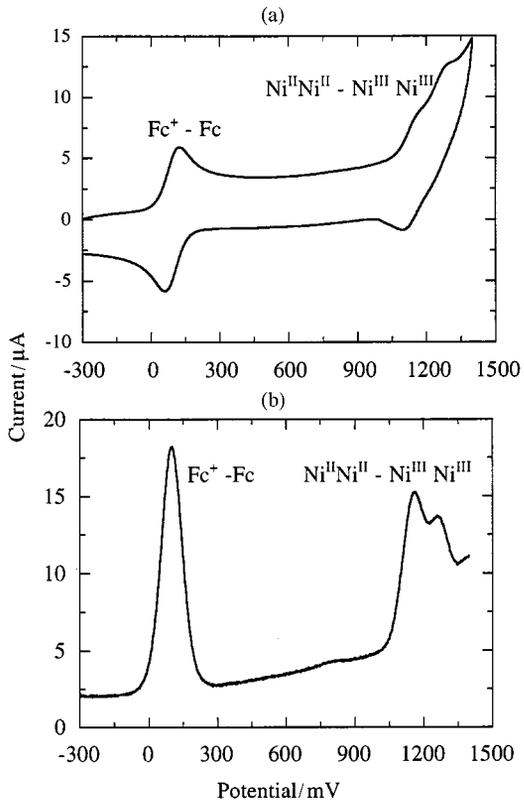

Fig. 3 Cyclic (a) and square-wave (b) voltammograms of complex **5**. Details as in Fig. 2.

SWV techniques shows that in this case (Table 4) the two $1e^-$ oxidation processes represented by eqn. (1) are separated by approximately 110 mV with $E_{\frac{1}{2}}$ values of +1.06 and +1.17 V. Thus, the first nickel(II) centre in **5** is oxidised to Ni^{III} at +1.06 V, which is almost the same average potential recorded for the two very closely spaced $1e^-$ oxidation processes of the complex of tmpdtnp, **2** (Table 4), while the second centre in **5** is harder than the first as evidenced by the value of +1.17 V. This behaviour parallels that of the analogous copper(II) complex which also showed two partially resolved electrochemical responses. In both complexes the electronic properties of the OH group of the propan-2-ol bridge influence the redox properties of the metal centres. For the nickel(II) complex, the central alcohol group of tmpdtnp-OH may be co-ordinating to the oxidised nickel(III) centre. This brings the two metal centres closer together and, consequently, the remaining nickel(II) centre becomes more difficult to oxidise.

The CV and SWV responses for complexes **2**–**4** (Fig. 4 displays data for **4**) are not even partially resolved like those of **1**. However, the value of $\Delta E_p = 80$–86 mV is considerably larger than that of approximately 30 mV expected for a simultaneous $2e^-$ oxidation step (*i.e.* 57 mV/*n* at 25 °C), indicating that two closely separated $1e^-$ oxidation processes having $E_{\frac{1}{2}}$ values separated by 30 ± 10 mV are occurring as shown in eqn. (1). The "average" $E_{\frac{1}{2}}$ values for **1**–**3** of +1.14, +1.07 and +1.06 V, respectively, become less positive with increasing length of the alkyl bridge used to link the two pentadentate ligand compartments (see Table 4). This trend has also been observed for the nickel(II) complexes of the corresponding alkyl bridged bis(cyclam) ligands studied by Ciampolini *et al.*[11] and was rationalised in terms of decreases in electrostatic repulsion between nickel centres with increasing M···M separation. This facilitates oxidation to the $Ni^{II}Ni^{III}$ and $Ni^{III}Ni^{III}$ states. At the extreme, the mononuclear complex, $[Ni(dmptacn)(OH_2)]^{2+}$, experiences a marked decrease in these electrostatic influences and is therefore more easily oxidised ($E_{\frac{1}{2}} = +0.98$ V[35]) than **1**–**3**. Notably, the minimised solution structures of the

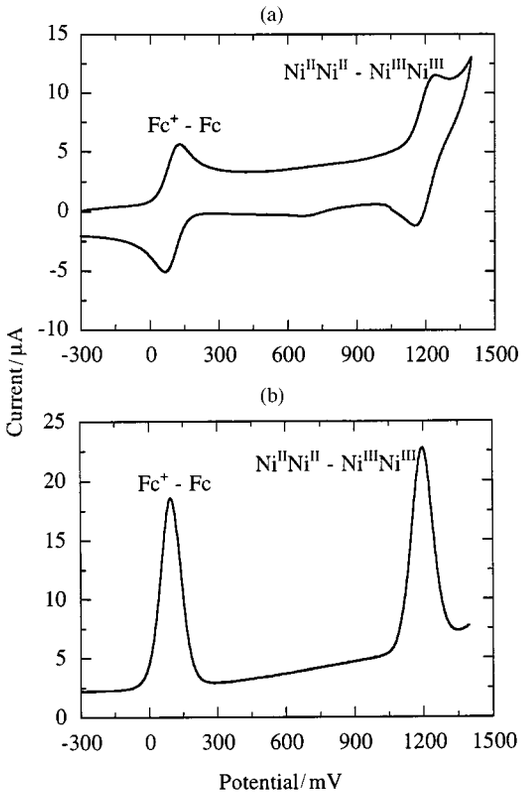

Fig. 4 Cyclic (a) and square-wave (b) voltammograms of complex **4**. Details as in Fig. 2.

copper(II) complexes of the ethane-, propane- and butane-bridged bis(pentadentate) ligands, *viz.* the analogues of **1**–**3**, confirmed an increase in M···M separation with alkyl chain length.[17] As was found here, the reduced Cu^ICu^I forms of these complexes are more easily oxidised as the M···M separation increases.

The nickel(II) complex of tmpdtn*m*-X, **4**, exhibits an $E_{\frac{1}{2}}$ value (+1.11 V) which is more positive than anticipated on the basis of the expected M···M separation, *i.e.* after resolved oxidation processes. This anomalous behaviour was also observed for the corresponding bis(cyclam) complexes where it was found that complexes of the *m*-xylene bridged ligand have a more positive $E_{\frac{1}{2}}$ value than those of the butane bridged ligand which has a shorter M···M separation.[11] In both systems, a combination of steric and inductive effects attributable to the xylene group could be reducing the donor strength of the bridgehead nitrogens compared to those with simple aliphatic substituents.[11] The decreased donor strength makes the oxidation of **4** more difficult and offsets the benefits of a decrease in the charge repulsion within the complex afforded by the larger Ni···Ni separation. The net result is that the $E_{\frac{1}{2}}$ value for **4** is more positive than that of **3**.

The square-wave data, after normalisation to a concentration of 5×10^{-4} mol dm^{-3} (Table 4), show the $1e^-$ ferrocene oxidation step produces a peak current/unit concentration value that is considerably larger than that of the partially resolved processes (**1**, **5**) and about the same as that of unresolved cases (**2**–**4**). However, analysis of the current magnitude of the square-wave currents using the theory reported in ref. 17 and assuming the diffusion coefficients are significantly less than that for ferrocene, as was demonstrated for the binuclear copper analogues, confirmed that the peak currents are of the correct magnitude for two unresolved or partially resolved $1e^-$ reversible charge transfer processes. Unfortunately, the inability to obtain quantitatively reliable CV or steady state data, due to the proximity of the background process, meant that more detailed calculations as presented for the copper system were not possible.

Conclusion

Studies of the co-ordination chemistry of a series of bis(pentadentate) ligands bearing 2-pyridylmethyl pendant groups have been extended to the nickel(II) complexes. Electrochemical analyses of these binuclear complexes established that the potentials associated with the oxidation processes decrease with the length of the alkyl group linking the two ligand compartments. This indicates an increase in Ni···Ni separation leads to a decrease in electrostatic repulsion in the oxidised state. For two complexes, **1** and **5**, splitting of the oxidation waves was clearly evident, confirming that two closely spaced $1e^-$ processes rather than a single $2e^-$ process were taking place (*i.e.* $Ni^{II}Ni^{II} \longrightarrow Ni^{II}Ni^{III} \longrightarrow Ni^{III}Ni^{III}$).

Acknowledgements

This work was supported by Australian Research Council grants to L. S. and A. M. B. S. J. B. was the recipient of a Monash Graduate Scholarship.

References

1 R. K. Thauer, G. Diekert and P. Schonheit, *Trends Biochem. Sci.*, 1980, **5**, 304.
2 J. O. Nriagu, *Nickel in the Environment*, Wiley, New York, 1980.
3 W. Mertz, *Science*, 1981, **213**, 1332.
4 F. W. Sunderman (Editor), *Nickel in the Human Environment*, Oxford University Press, New York, 1985, p. 530.
5 M. A. Halcrow and G. Christou, *Chem. Rev.*, 1994, **94**, 2421; A. F. Kolodziej, *Prog. Inorg. Chem.*, 1994, **41**, 493.
6 E. Jabri, M. B. Carr, R. P. Hausinger and P. A. Karplus, *Science*, 1995, **268**, 998; D. E. Wilcox, *Chem. Rev.*, 1996, **96**, 2435.
7 A. Volbeda, M.-H. Charon, C. Piras, E. C. Hatchikian, M. Frey and J. C. Fontecilla-Camps, *Nature*, (*London*), 1995, **373**, 580.
8 See, for example, L. Sacconi, F. Mani and A. Bencini, in *Comprehensive Coordination Chemistry*, eds. G. Wilkinson, R. D. Gillard and J. A. McCleverty, Pergamon Press, Oxford, 1987, vol. 5, p. 1; V. McKee, *Adv. Inorg. Chem.*, 1993, **40**, 323; D. E. Fenton and H. Okawa, *Chem. Ber.*, 1997, **130**, 433; D. Volkmer, B. Hommerich, K. Griesar, W. Haase and B. Krebs, *Inorg. Chem.*, 1996, **35**, 3792 and refs. therein.
9 P. D. Beer, M. G. B. Drew, P. B. Leeson, K. Lyssenko and M. I. Ogden, *J. Chem. Soc.*, *Chem. Commun.*, 1995, 929.
10 G. A. McLachlan, G. D. Fallon, R. L. Martin, B. Moubaraki, K. S. Murray and L. Spiccia, *Inorg. Chem.*, 1994, **33**, 4663.
11 M. Ciampolini, L. Fabbrizzi, A. Perotti, A. Poggi, B. Seghi and F. Zanobini, *Inorg. Chem.*, 1987, **26**, 3527.
12 K. Wieghardt, I. Tolksdorf and W. Herrmann, *Inorg. Chem.*, 1985, **24**, 1230.
13 B. Graham, G. D. Fallon, M. T. Hearn, D. C. R. Hockless, G. Lazarev and L. Spiccia, *Inorg. Chem.*, 1997, **36**, 6366.
14 W. B. Tolman, *Acc. Chem. Res.*, 1997, **30**, 227; S. Mahapatra, S. Kaderli, A. Llobet, Y.-M. Neuhold, T. Palanche, J. A. Halfen, V. G. Young, Jr., T. A. Kaden, L. Que, Jr., A. D. Zuberbuhler and W. B. Tolman, *Inorg. Chem.*, 1997, **36**, 6343.
15 A. J. Blake, T. M. Donlevy, P. A. England, I. A. Fallis, S. Parsons, S. A. Ross and M. Schroder, *J. Chem. Soc.*, *Chem. Commun.*, 1994, 1981.
16 S. J. Brudenell, L. Spiccia and E. R. T. Tiekink, *Inorg. Chem.*, 1996, **35**, 1974.
17 S. J. Brudenell, L. Spiccia, A. M. Bond, P. Comba and D. C. R. Hockless, *Inorg. Chem.*, 1998, **37**, 3705.
18 F. H. Fry, B. Graham, L. Spiccia, D. C. R. Hockless and E. R. T. Tiekink, *J. Chem. Soc.*, *Dalton Trans.*, 1997, 827.
19 XDISK, *Data Reduction Program*, Version 4.20.2PC, Siemens Analytical X-Ray Instruments, Inc., Madison, WI, 1989.
20 N. Walker and D. Stuart, *Acta Crystallogr.*, *Sect. A*, 1983, **39**, 158.
21 SIR 92, A. Altomare, M. Cascarano, C. Giacovazzo and A. Guagliardi, *J. Appl. Crystallogr.*, 1993, **26**, 343.
22 DIRDIF 94, P. T. Beurskens, G. Admiraal, G. Beurskens, W. P. Bosman, R. de Gelder, R. Israel, R. O. Gould and J. M. M. Smits, *The DIRDIF-94 Program System*, Technical Report of the Crystallography Laboratory, University of Nijmegen, 1994.
23 D. T. Cromer and J. T. Waber, *International Tables for X-Ray Crystallography*, Kynoch Press, Birmingham, 1974, Table 2.3.A.
24 J. A. Ibers and W. C. Hamilton, *Acta Crystallogr.*, 1964, **17**, 781.
25 TEXSAN, Crystal Structure, Analysis Package, Molecular Structure Corporation, Houston, TX, 1992.

26 C. K. Johnson, ORTEP, Report ORNL-5138, Oak Ridge National Laboratory, Oak Ridge, TN, 1976.
27 K. Wasielewski and R. Z. Mattes, *Z. Anorg. Allg. Chem.*, 1993, **619**, 158.
28 K. Wieghardt, U. Bossek, P. Chaudhuri, W. Herrmann and H. J. Kueppers, *Inorg. Chem.*, 1982, **21**, 4308.
29 M. J. Van der Merwe, J. C. A. Boeyens and D. R. Hancock, *Inorg. Chem.*, 1985, **24**, 1208.
30 S. J. Brudenell, L. Spiccia, A. M. Bond, G. D. Fallon, D. C. R. Hockless and E. R. T. Tiekink, unpublished work.
31 D. Sutton, *Electronic Spectra of Transition Metal Complexes*, McGraw-Hill, London, 1968.
32 S. M. Hart, J. C. Boeyens and R. D. Hancock, *Inorg. Chem.*, 1983, **22**, 982.
33 R. Stranger, S. C. Wallis, L. R. Gahan, C. H. L. Kennard and K. A. Byriel, *J. Chem. Soc.*, *Dalton Trans.*, 1992, 2971.
34 A. Urfer and T. A. Kaden, *Helv. Chim. Acta*, 1994, **77**, 23.
35 G. A. McLachlan, Ph.D. Thesis, Monash University, Melbourne, 1994.
36 K. Wieghardt, E. Schoffman, B. Nuber and J. Weiss, *Inorg. Chem.*, 1986, **25**, 877.
37 R. Yang and L. J. Zompa, *Inorg. Chem.*, 1976, **15**, 1499.

Paper 8/06084C